

Optical Bistability in a Traveling-Wave SOA Connected to a DFB Laser Diode: Theory and Experiment

Wouter D'Oosterlinck, *Student Member, IEEE*, Geert Morthier, *Senior Member, IEEE*,
Roel Baets, *Senior Member, IEEE*, and Thomas Erneux

Abstract—We investigate the bistable response of a traveling-wave semiconductor optical amplifier (SOA) connected bidirectionally to a distributed feedback (DFB) laser diode. By contrast to dispersive DFB amplifiers, bistability is possible for a broad wavelength range of the injected optical signal. A theoretical analysis clarifies the origin of the phenomenon and the conditions under which it occurs. Numerical simulations and experimental results confirm the theoretical analysis. Experimentally obtained step heights up to 25 dB and widths of the bistability domain of 1–4 dB have been found.

Index Terms—Optical bistability, optical signal processing, semiconductor optical amplifier (SOA).

I. INTRODUCTION

IT IS expected that, at least to some degree, the future all-optical networks will be based on some form of optical packet or optical burst switching, with the routing and forwarding being implemented all-optically. For such networks, and especially for the processing of optical labels or optical headers, there is a need for all-optical flip-flops, in which a certain output state (e.g., determining the routing) can be set from a short input pulse (e.g., derived from a header) and in which this output state is maintained until a reset pulse is applied. In essence, such flip-flops are based on bistable devices, which for certain operation conditions can operate in one of two stable states.

In recent years, several valuable solutions for all-optical flip-flops or bistable devices have been proposed. One of the earliest known bistable devices (see, e.g., [1] and [2]) is a distributed feedback (DFB) amplifier, which shows dispersive hysteresis for signal wavelengths in the very close proximity of the resonance wavelengths. More recently (see, e.g., [3], [4]), pairs of mutually coupled and equally pumped laser diodes

have been proposed. In these configurations and depending on the history, one of both coupled lasers is lasing and suppresses the other laser. The two output states are then typically corresponding with different wavelengths, but exhibit equal output power. Also a single, semiconductor optical amplifier (SOA)-based Mach-Zehnder interferometer with a feedback loop has recently been proposed as an all-optical flip-flop [5]. Due to the fact that the operation is essentially based on interference in this case, the device requires a careful operation.

Here, we propose another device that can exhibit bistable behavior: a traveling-wave SOA bidirectionally coupled to a DFB laser diode. By contrast to dispersive DFB amplifiers, the bistability is obtained over a very broad wavelength range for the injected lightwave. The bistability is observed in both the output power of the SOA and (inverted) in the output power of the laser diode. It is possible to design the device such that the bistability becomes independent of the input polarization. Both the set and the reset pulses can also be optical pulses. The device that we propose is therefore quite robust and flexible. The fact that the input power can originate from an isolated (e.g., distant) laser, implies that this isolated laser can be independently controlled, a feature that could be of importance when one thinks of using, e.g., a tunable laser for the generation of the input power.

A similar structure has been proposed in [6]. However, the DFB in [6] is a DFB amplifier, i.e., biased below threshold, and the traveling-wave SOA just acts as a booster amplifier. The bistability observed in [6] is the dispersive bistability in a DFB amplifier, which is obtained for input wavelengths close to the resonance wavelengths of the DFB structure. In the device that we propose, the DFB is biased above threshold and the bistable behavior depends on the nonlinear interaction between the SOA and the DFB laser diode.

The paper is organized as follows. In Section II, we will introduce the device structure and the principle nonlinearity responsible for the bistable behavior. In Section III, a theoretical analysis is presented that allows to determine how the hysteresis depends on the operating conditions. Section IV gives numerical simulation results, and in Section V, we present an experimental confirmation of the theoretical and numerical analysis.

II. DEVICE DESCRIPTION AND ORIGIN OF BISTABLE BEHAVIOR

The device that we consider is in essence a traveling-wave SOA connected to an AR-coated DFB laser diode, as shown schematically in Fig. 1. The device can be implemented in a

Manuscript received February 13, 2006; revised April 3, 2006. This work was supported by the InterUniversity Attraction Pole of the Belgian government and by the Fonds National de la Recherche Scientifique (Belgium). The work of W. D'Oosterlinck was supported by the Institute for the Promotion of Innovation through Science and Technology in Flanders (IWT-Vlaanderen) under a specialization grant.

W. D'Oosterlinck, G. Morthier, and R. Baets are with the Photonics Research Group, Department of Information Technology (INTEC), Ghent University-IMEC, 9000 Ghent, Belgium (e-mail: wouter.doosterlinck@intec.ugent.be; morthier@intec.UGent.be; Roel.Baets@intec.UGent.be).

T. Erneux is with the Theoretical Nonlinear Optics Department, Free University of Brussels, B-1050 Brussels, Belgium (e-mail: terneux@ulb.ac.be).

Digital Object Identifier 10.1109/JQE.2006.877295

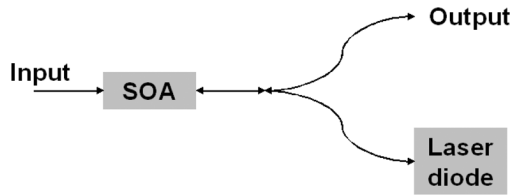


Fig. 1. Schematic of a semiconductor laser integrated with an SOA.

hybrid or an integrated version. This device has been presented previously as a 2R optical signal regenerator [7], and here we demonstrate that it can also exhibit a bistable response under the appropriate operating conditions.

The bistable behavior occurs if the SOA is pumped sufficiently strong and/or if the laser power is sufficiently low. It can be attributed to the fact that for these operation conditions and for certain input power levels to the SOA there exist two stable states. In the first state, the SOA gives a relatively large amplification and its output switches off the laser diode (due to the amplified external light). In the second state, the SOA gives a relatively smaller amplification and its output is insufficient to switch off the laser diode. The small amplification is a consequence of the saturation of the SOA by the laser diode power. The bistable behavior is then observed in both the output power at the input signal wavelength and in the output from the laser diode.

Of particular interest is the fact that the bistable behavior normally occurs for any input signal wavelength and is fairly wavelength independent as long as this wavelength is not close to the Bragg wavelength of the DFB laser.

It is important that unwanted reflections in the device are minimized by using AR-coated facets at both sides of the device (SOA front facet and laser diode back facet), such that the amplified signal is not reflected back in the laser diode and the SOA. For a hybrid device AR-coatings are required on all facets. As we have already mentioned, the wavelength of the injected light should be sufficiently distant from the lasing wavelength such that the laser diode acts as a traveling-wave amplifier for the signal light. If the wavelength of the injected light is too close to the lasing wavelength, the signal injected into the laser diode starts resonating in the DFB cavity and is reflected back into the SOA. The strong reflected signal injected on the right-hand side of the SOA then implies that the SOA is always in a saturated low-amplification regime with the amplified signal unable to switch off the laser diode. However, instead of an AR-coated DFB laser, one could also use an AR-coated DBR laser with Bragg reflectors on either side of the gain section.

In the device shown in Fig. 1, the ON state for the signal power (corresponding with the laser in the OFF state) can be set by injecting an optical pulse on top of the continuous wave (CW) power needed to operate the device in the bistable domain from the left-hand side. The OFF state for the signal power (corresponding with the laser in the ON state) can be reset by injecting an optical pulse in the upper waveguide on the right-hand side (where it is denoted “output power” in Fig. 1).

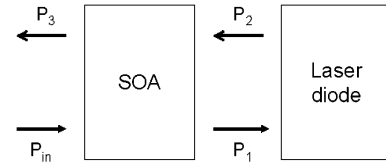


Fig. 2. Model and notations used in the analytical analysis.

III. THEORETICAL ANALYSIS

The bistable behavior can be described analytically using a simple steady-state model. Specifically, we consider a traveling wave SOA connected to a DFB laser diode as shown in Fig. 2.

In this model, reflections from the signal light back into the SOA as well as reflections of the laser signal back into the laser diode are neglected. Therefore, P_{in} and P_1 are considered to be at the signal wavelength while P_2 and P_3 are considered to be at the laser wavelength.

Because the wavelength of the injected light is substantially different from the DFB lasing wavelength, the effect of the feedback is essentially incoherent. If the laser output is nonzero and provided the injected signal is sufficiently weak, the steady-state carrier density in the DFB laser is not perturbed by the feedback. From the steady-state carrier density equation, we have $P_{las} - c(P_2 + P_1) = 0$ if $P_2 \neq 0$ where P_{las} is the laser power without injection and c is a dimensionless coefficient. Since we only consider the steady-state problem, c can be removed by properly redefining P_{las} . This then leads to the simple model equations

$$P_2 = P_{las} - P_1 \text{ if } P_1 \leq P_{las} \quad (1)$$

$$= 0 \text{ if } P_1 > P_{las} \quad (2)$$

where $P_{las} > 0$ denotes the laser power without injection. The SOA is described in terms of the forward and backward propagating powers P_+ and P_- , respectively [8]. From the steady-state traveling-wave equations, we have the following equations for P_+ and P_- :

$$\frac{dP_+}{dz} = (g - \alpha_{int})P_+ \quad (3)$$

$$\frac{dP_-}{dz} = -(g - \alpha_{int})P_- \quad (4)$$

where $g(N)$ is the local gain power and α_{int} is the SOA internal loss coefficient. $g(N)$ is approximated as $g = \Gamma a(N - N_0)$, where Γ is the confinement factor that takes into account the transverse effects, N_0 is the carrier density at transparency, and a is the gain coefficient. The steady-state carrier density equation is given by [8]

$$\frac{I}{qV} = \frac{N}{\tau_c} + \frac{g(N)}{\hbar\omega_0 v d} (P_+ + P_-) \quad (5)$$

where I is the injection current, q is the electron charge, V is the active volume, τ_c is the spontaneous carrier lifetime, $\hbar\omega_0$ is

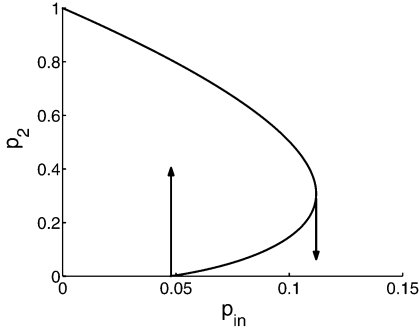


Fig. 3. Normalized feedback power p_2 as a function of the normalized injected power for $p_{\text{las}} = 1$ and $g_0 L = 4$.

the photon energy, w is the width of the active region, and d is the thickness of the active layer. In this paper, we consider the simplified case $\alpha_{\text{int}} = 0$. It is not a limitation of our analysis but with $\alpha_{\text{int}} = 0$, two solutions, one with $P_2 \neq 0$ and one with $P_2 = 0$ immediately emerge. The detailed analysis is given in Appendix I, and the general case $\alpha_{\text{int}} \neq 0$ will be treated elsewhere [].

With all powers normalized by the saturation power $P_{\text{sat}} \equiv \hbar\omega_0 w d / (a\Gamma\tau_c)$, the solution $p_2 \equiv P_2/P_{\text{sat}} \neq 0$ satisfies the following transcendental equation:

$$g_0 L = \ln\left(\frac{p_{\text{las}} - p_2}{p_{\text{in}}}\right) + p_2 \left(\frac{p_{\text{las}} - p_2}{p_{\text{in}}} - 1\right) - p_{\text{in}} + p_{\text{las}} - p_2 \quad (6)$$

where $p_{\text{in}} \equiv P_{\text{in}}/P_{\text{sat}}$ and $p_{\text{las}} \equiv P_{\text{las}}/P_{\text{sat}}$. g_0 is defined in Appendix I as the unsaturated gain of the SOA which is proportional to the injection current I . L is the length of the SOA. In this regime, the laser is not switched off and $p_1 \equiv P_1/P_{\text{sat}} = p_{\text{las}} - p_2$. As p_2 increases, the SOA is progressively saturated and the amplification p_1/p_{in} decreases. The second solution corresponds to $p_2 = 0$ and p_1 satisfying

$$\ln\left(\frac{p_1}{p_{\text{in}}}\right) + \frac{1}{p_{\text{sat}}}(p_1 - p_{\text{in}}) = g_0 L. \quad (7)$$

In this regime, the amplification p_1/p_{in} for the input signal is much larger because the laser is switched off. The normalized feedback power p_2 (Fig. 3) and signal power p_1 (Fig. 4) are represented as functions of the normalized injected power for $p_{\text{las}} = 1$ and $g_0 L = 4$. They have been obtained by solving numerically (6) and (7). Note that p_1 is given by (7) only for $p_1 > p_{\text{las}}$.

By analyzing (6) for small values of p_2 , we may find the condition for a Z-shaped diagram for $p_2 = p_2(p_{\text{in}})$. This condition is given by

$$g_0 L > \ln\left(\frac{1 + 2p_{\text{las}}}{p_{\text{las}}}\right) + p_{\text{las}} \frac{1 + p_{\text{las}}}{1 + 2p_{\text{las}}}. \quad (8)$$

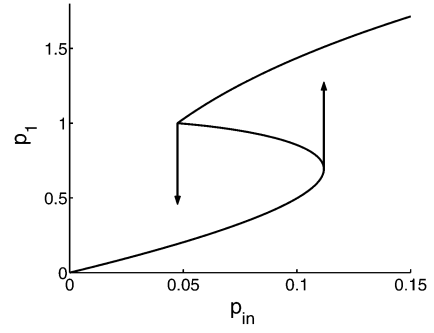


Fig. 4. Normalized feedback power p_1 as a function of the normalized injected power for $p_{\text{las}} = 1$ and $g_0 L = 4$.

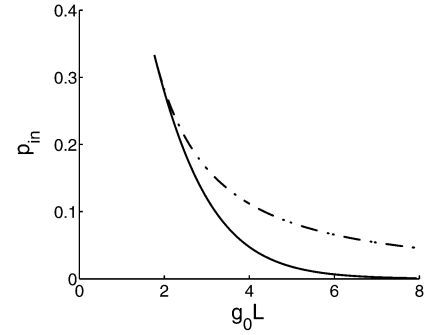


Fig. 5. Evolution of the left and right boundary for p_{in} of the hysteresis loop as a function of $g_0 L$ for $p_{\text{las}} = 1$.

The inequality (8) clearly indicates that the unsaturated amplification of the SOA needs to surpass a threshold value determined by the laser output power without injection, p_{las} . Equivalently, the bias to the laser diode has to be sufficiently low. The width of the bistability domain can be determined analytically. The left boundary is obtained from (6) with $p_2 = 0$, and the right boundary is obtained from (7) and the extra condition $dp_{\text{in}}/dp_1 = 0$, as can be seen in Appendix II. In Fig. 5, the evolution of the width of the bistability domain is shown as a function of $g_0 L$. It shows that the width of the bistability domain increases with increasing values of $g_0 L$ (or equivalently with decreasing values of p_{las}).

One can do a similar analysis when a certain coupling efficiency between SOA and DFB laser is assumed (if for instance the DFB laser diode and SOA are connected through a coupler as in Fig. 1 instead of just butt coupled as in Fig. 2). The formulas become then more complicated and will not be given here []. However, they indicate that with decreasing coupling efficiency, the bistability starts at ever increasing amplifier gain. For too low coupling efficiencies, the required amplifier gain is so large that it cannot be achieved practically (e.g., due to heating, saturation or lasing problems).

IV. NUMERICAL SIMULATIONS

Using a commercial software package [9], the static behavior of the proposed device was investigated. The scheme we used consisted of a bulk traveling-wave SOA and a quarter wave shifted DFB laser diode that are connected through a bidirectional coupler. Both the laser diode and the SOA are assumed to

TABLE I
DEVICE PROPERTIES OF THE SCHEME USED IN THE SIMULATIONS

SOA chip length	500 μm
Laser chip length	350 μm
Active region width	2.5 μm
Active region thickness	0.2 μm
Confinement factor laser diode	0.3
Confinement factor SOA	0.45
Laser wavelength	1552.5 nm
Signal wavelength	1537.4 nm

TABLE II
DEFAULT PARAMETERS OF THE SOFTWARE PACKAGE USED FOR THE NUMERICAL SIMULATIONS

Internal loss	$30 \frac{1}{\text{cm}}$
Index grating coupling coefficient	$60 \frac{1}{\text{cm}}$
Linear material gain coefficient	$3e^{-16} \text{cm}^2$
Non-linear material gain coefficient	$10e^{-17} \text{cm}^3$
Material linewidth enhancement factor	3
Population inversion factor	1

have AR coatings at both facets. Some typical device parameters used in the simulations are shown in Table I. Other important parameters were default parameters from the software package and are shown in Table II.

The scheme used in these simulations is the same as the one in Fig. 1. Light is injected at the front facet of the SOA and after travelling through the SOA, part of the light is injected into the laser diode. The remaining part of the output light is extracted as well as the laser signal that travels back to the SOA. For these simulations the coupling factor between laser diode and SOA was kept constant at 0.5 thus assuming the use of a 3-dB coupler between the SOA and the laser.

In Fig. 6, the behavior of the output power of the laser (corresponding to p_2 in the theoretical analysis) is given as a function of the input power to the SOA for different combinations of the supply currents for SOA and laser diode. In agreement with the theoretical analysis, it can be seen that the gain of the SOA (or the current of the SOA) needs to be sufficiently high, with the threshold for bistability depending on the laser power or the laser current. The decision point shifts to higher input powers for increasing laser currents (or decreasing SOA currents) as could be expected. It can also be seen that, in agreement with Fig. 5, the width of the hysteresis loop increases with increasing SOA supply current (for constant laser supply current) or decreasing laser supply current (for constant SOA supply current). The bistability in the laser output power corresponds with an extinction ratio of over 20 dB and the width of the hysteresis varies between 0 and 4 dB.

Fig. 7 shows the output power of the SOA (corresponding to p_1 in the theoretical analysis) as a function of the input power to the SOA for an SOA current of 100 mA and different supply currents for the laser diode. These graphs are approximately inverted versions of the corresponding ones in Fig. 6 indicating a strong interaction between the signal light and the laser light. This time, the step is directed towards higher output powers, and step heights of up to about 8 dB can be achieved. The width of the hysteresis is of course the same as in Fig. 6.

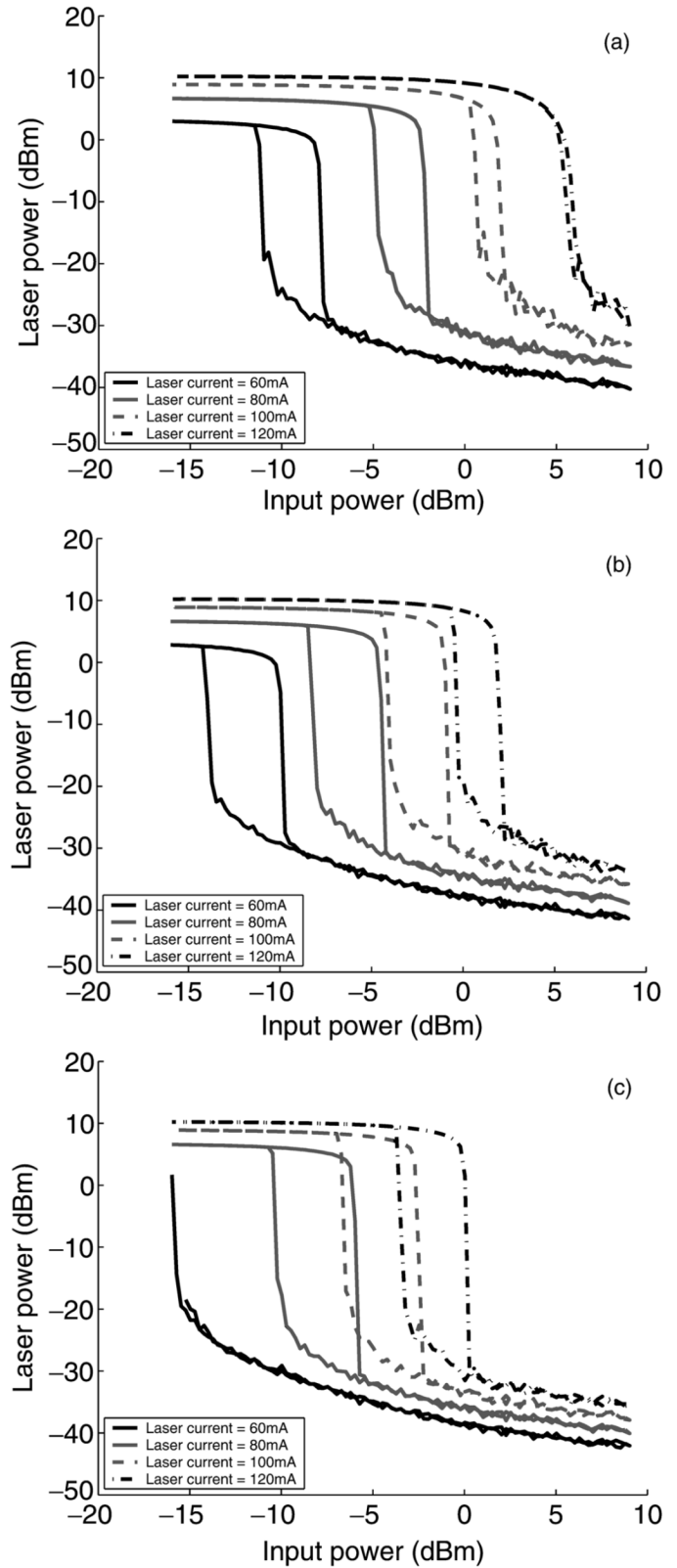


Fig. 6. Output power of the laser diode as a function of the input power to the SOA for different supply currents to the laser diode (see legend) and different supply currents to the SOA. (a) 80 mA. (b) 100 mA. (c) 120 mA.

Simulations with different coupling ratios indicate that the higher the coupling ratio, the stronger the interaction between SOA and laser diode becomes. In Fig. 8, the laser power is

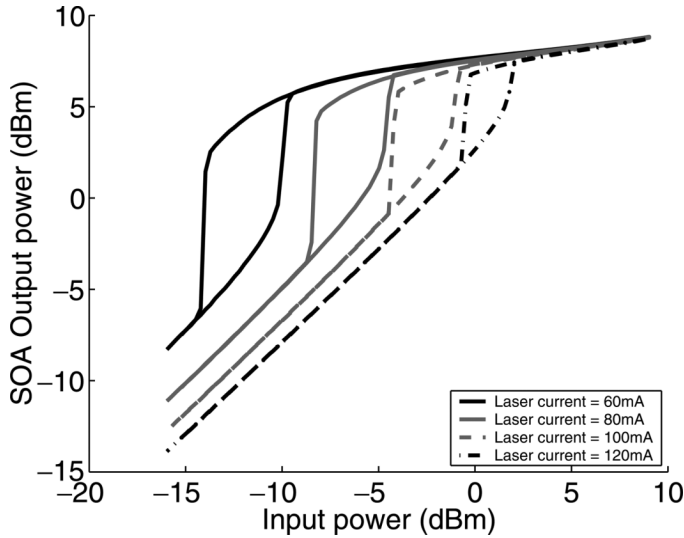


Fig. 7. Output power after the SOA as a function of the input power to the SOA for different supply currents to the laser diode (see legend) and a supply current to the SOA of 100 mA.

shown as a function of the input power for a coupling ratio of 0.2 and 0.75, respectively. In both cases, the supply current to the SOA was 120 mA. One can clearly see that to obtain proper operation within a reasonable input power region, the coupling ratio has to be sufficiently high. The influence of higher coupling ratios than in Fig. 6, however, seems limited as can also be seen from the theoretical analysis when a certain coupling efficiency between laser diode and SOA is taken in to account.

V. EXPERIMENTAL RESULTS

Using a wavelength selectable light source [10] consisting of an SOA with an angled output waveguide, followed by a 4X1-MMI optical coupler and 4 ($\lambda/4$)-shifted DFB laser diodes with straight output waveguides, the working principle of the proposed device has been investigated experimentally. A schematic representation of the device is given in Fig. 9. The four DFB laser diodes each operate at a different wavelength and can be temperature tuned. For our purpose only, one of the lasers will be used. This results in a coupling ratio of 0.25 between the SOA and the laser diode. Light from a tunable laser is amplified with an EDFA and injected into the SOA. The output signal can be extracted at both sides of the component, but due to the optimized coupling at the angled SOA facet the output power is extracted there. A circulator is then used to separate the output signal from the input signal. Furthermore, only the laser signal is investigated experimentally because of the low reflection for the input signal from the back facet. The wavelength of the laser diode is fixed at 1540 nm, and the drive current for the laser diode is fixed at 87 mA. No polarization influence has been observed during these measurements.

In Fig. 10 operation of the device for different input signal wavelengths is shown. For the same SOA current (100 mA) good operation over a wavelength range of about 12 nm is shown, with step heights up to 25 dB and bistability widths between 1 and 3 dB. The difference between the different

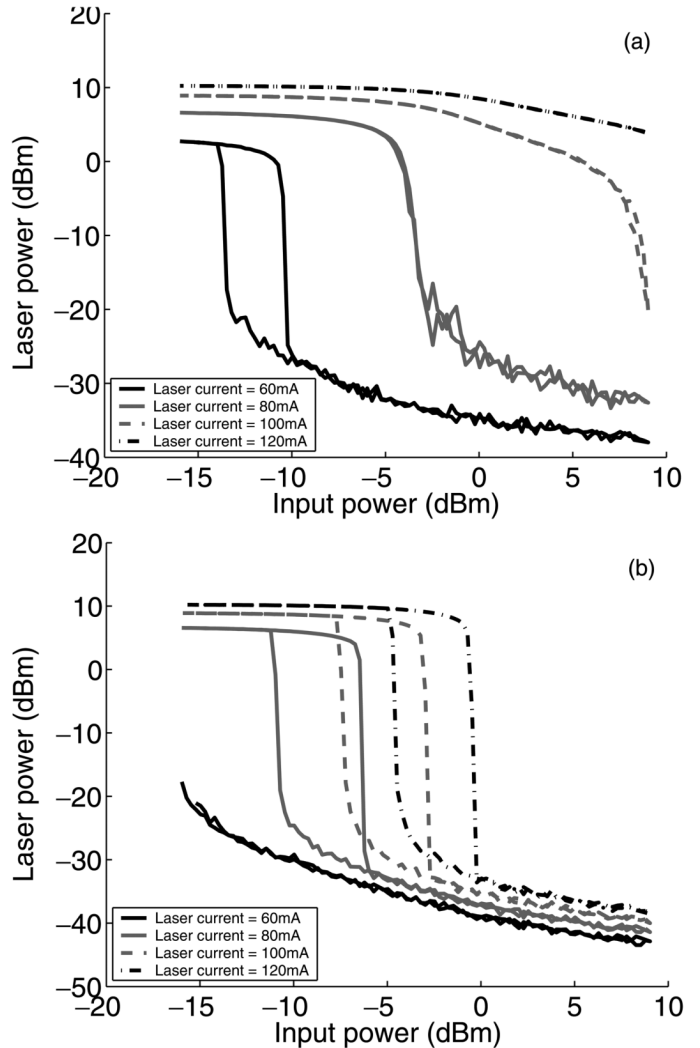


Fig. 8. Laser power as a function of the input power to the SOA for a supply current to the SOA of 120 mA, a coupling ratio of (a) 0.2 or (b) 0.75 and different supply currents to the laser diode (see legend).

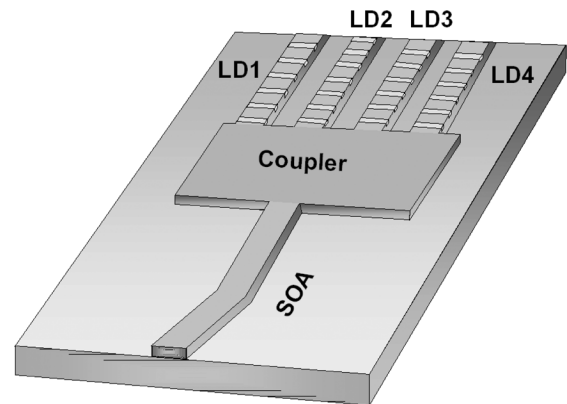


Fig. 9. Schematic representation of the device used in the experiments.

wavelengths can be sought in the difference in gain and coupling into the grating of the laser diode at the different signal wavelengths. For signal wavelengths close to the central Bragg wavelength of the laser signal light couples into the grating disturbing the feedback between laser diode and SOA. These

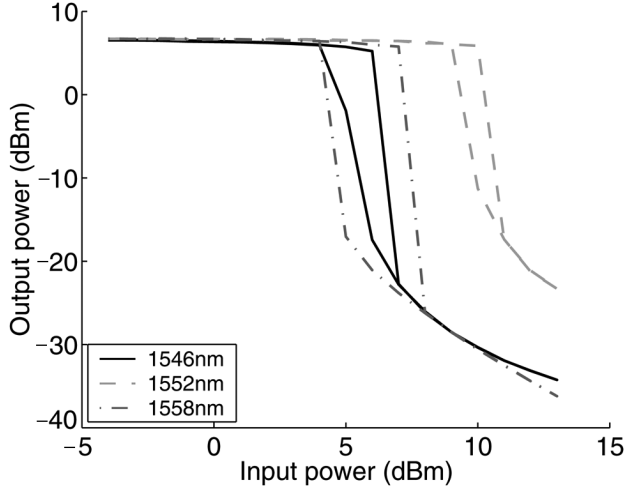


Fig. 10. Measured output versus input power relation for different wavelengths for the input signal.

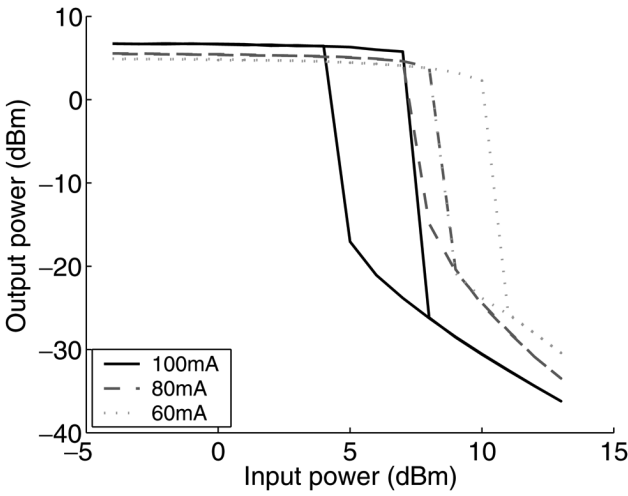


Fig. 11. Measured output versus input power relation for different SOA currents.

measurements were limited by the available optical filters, but it is expected, as has also been seen in simulations, that good operation over a broader wavelength region is feasible.

In addition to the wavelength dependence, we also looked into the adjustability of the hysteresis of the device by adjusting only the drive current of the SOA. For these measurements the signal wavelength was set at 1555 nm. As shown in Fig. 11, step heights of about 25 dB and bistability widths of 1–4 dB can again be achieved.

Comparing Fig. 11 with Fig. 6, a good agreement between the numerical simulations and experimental results can be found. In both cases, it can be seen that the input power for which the step occurs decreases for higher SOA drive currents with constant laser drive currents. Using the wavelength dependence of the device shown in Fig. 10 and the tunability shown in Fig. 11, the same device could be used for several different wavelength channels with near identical operation characteristics. Considering the fact that the speed of this device is primarily determined by the feedback time between the SOA and the laser diode, it is believed that with this integrated device

high switching speeds can be obtained. A single feedback time for a device with a typical length of under 1 mm is of the order of 10 ps and the total feedback time is then determined by the feedback strength (depending on the effect a change in output power of one of the two components has on the other).

VI. CONCLUSION

We have discussed a new type of optical bistable behavior in a TW-SOA connected to a DFB laser diode. The bistability can be obtained for a broad range of input signal wavelengths and can be adjusted by simply changing the currents injected into the SOA and the DFB laser diode. The laser diode must have AR-coated facets, but does not need to be a DFB laser diode. A DBR laser diode (e.g., a widely tunable SG-DBR laser) with two AR-coated facets and Bragg sections on either side of the gain section can also be used. Moreover, both hybrid and integrated implementations of the device can be used. We have obtained excellent agreement between the theoretical analysis and the numerical and experimental results. Very steep steps in the output power of up to 25 dB have been observed in the output power of the laser as well as a rather narrow bistability region. The device is a relatively simple, robust, and flexible component, which could be used in a variety of applications and is in principle also suitable as an optically settable and resettable flip-flop.

APPENDIX I

DERIVATION OF THE ANALYTICAL RESULTS

It is mathematically more convenient to rewrite (5) in terms of the gain $g = \Gamma a(N - N_0)$. Equations (3) and (4) then become

$$\frac{dP_+}{dz} = (g - \alpha_{\text{int}})P_+ \quad (9)$$

$$\frac{dP_-}{dz} = -(g - \alpha_{\text{int}})P_- \quad (10)$$

$$\frac{g_0 - g}{\tau_c} = \frac{g}{E_{\text{sat}}}(P_+ + P_-) \quad (11)$$

$$P_+(0) = P_{\text{in}}, \quad P_-(L) = P_2 \quad (12)$$

where

$$g_0 \equiv \Gamma a N_0 \left(\frac{I}{I_0} - 1 \right) \quad E_{\text{sat}} \equiv \frac{\hbar \omega_0 w d}{\Gamma a} \quad (13)$$

and $I_0 \equiv qV N_0 \tau_c^{-1}$ is the current required for transparency. Equations (1) and (2) describes the effect of the feedback. We need to solve (9)–(12) separately for $P_1 \leq P_{\text{las}}$ and $P_1 > P_{\text{las}}$. The second problem is easier because $P_2 = 0$, but it is the first problem where $P_2 \neq 0$ that captures the hysteresis phenomenon. For mathematical clarity, we assume $\alpha_{\text{int}} \ll g$. It is not a limitation of our analysis but it considerably simplifies the algebra.

Considering the first problem we obtain from (9) and (11)

$$P_+ P_- = C \quad (14)$$

where C is a constant to be determined. Using (1), we eliminate P_+ in the remaining equations. After some calculations, we obtain a first order differential equation for P_- given by

$$P'_- = -\frac{g_0 P_-^2}{P_- + \frac{(P_-^2 + C)}{P_{\text{sat}}}}. \quad (15)$$

This equation is separable and integrating with the boundary condition $P_-(L) = P_2$ leads to the following solution (in implicit form):

$$-g_0(z-L) = \frac{1}{P_{\text{sat}}} \left[(P_- - P_2) - C \left(\frac{1}{P_-} - \frac{1}{P_2} \right) \right] + \ln \left(\frac{P_-}{P_2} \right). \quad (16)$$

Evaluating this equation at $z = 0$ and making use of (1) we obtain the following equation for P_2 :

$$g_0 L = \frac{1}{P_{\text{sat}}} \left[P_2 \left(\frac{P_{\text{las}} - P_2}{P_{\text{in}}} - 1 \right) - (P_{\text{in}} - P_{\text{las}} + P_2) \right] + \ln \left(\frac{P_{\text{las}} - P_2}{P_{\text{in}}} \right). \quad (17)$$

Normalizing all powers by P_{sat} , (17) becomes

$$g_0 L = \ln \left(\frac{p_{\text{las}} - p_2}{p_{\text{in}}} \right) + p_2 \left(\frac{p_{\text{las}} - p_2}{p_{\text{in}}} - 1 \right) - p_{\text{in}} + p_{\text{las}} - p_2 \quad (18)$$

where $p_j = P_j/P_{\text{sat}}$. By using $p_2 = p_{\text{las}} - p_1$ one finds an equation for p_1 as a function of p_{in}

$$\ln \left(\frac{p_1}{p_{\text{in}}} \right) + (p_{\text{las}} - p_1) \left(\frac{p_1}{p_{\text{in}}} - 1 \right) - p_{\text{in}} + p_1 = g_0 L. \quad (19)$$

Equation (18) is a transcendental equation for p_2 which is easy to analyze if we consider the length as the control parameter. There is a bifurcation point at $L = L_c$ where $p_2 = 0$ which is given by

$$L_c = g_0^{-1} \left[\ln \left(\frac{p_{\text{las}}}{p_{\text{in}}} \right) - p_{\text{in}} + p_{\text{las}} \right]. \quad (20)$$

The bifurcation diagram admits either one or two nonzero solutions for p_2 . The condition for two nonzero solutions implies hysteresis. It is obtained by determining the direction of bifurcation at $L = L_c$. Expanding (18) for small p_2 and small $L - L_c$, we find that $L - L_c > 0$ if

$$-\frac{1}{p_{\text{las}}} + \frac{p_{\text{las}}}{p_{\text{in}}} - 2 > 0. \quad (21)$$

Equation (21) is the condition for hysteresis which depends on p_{las} and p_{in} . It is satisfied for sufficiently low values of p_{in} . If we consider p_{in} as our control parameter, as it is the case in our experiments, then we need to solve (18) numerically as can be seen in Figs. 3 and 4.

Rewriting (21) gives us

$$p_{\text{in}} < \frac{p_{\text{las}}^2}{2p_{\text{las}} + 1}. \quad (22)$$

And substituting this in (18) then results in a condition for $g_0 L$ as a function of p_{las}

$$g_0 L > \ln \left(\frac{1 + 2p_{\text{las}}}{p_{\text{las}}} \right) + p_{\text{las}} \frac{1 + p_{\text{las}}}{1 + 2p_{\text{las}}}. \quad (23)$$

Finally, we repeat the analysis for the second problem where $P_2 = 0$. We find

$$\ln \left(\frac{P_1}{P_{\text{in}}} \right) + \frac{1}{P_{\text{sat}}} (P_1 - P_{\text{in}}) = g_0 L \quad (24)$$

which is an equation for P_1 . Our solution is valid until $P_1 = P_{\text{las}}$. Substituting $P_1 = P_{\text{las}}$ into (24) leads again to the critical length $L = L_c$ given by (20). Normalizing again all powers in (24) by P_{sat} yields

$$\ln \left(\frac{p_1}{p_{\text{in}}} \right) + (p_1 - p_{\text{in}}) = g_0 L. \quad (25)$$

APPENDIX II

WIDTH OF THE HYSTERESIS LOOP

When looking at the width of the hysteresis loop one finds that there are two boundaries for this loop. The first being determined by the condition $p_2 = 0$ as can also be seen from (20). Rewriting this as a function of p_{las} and $g_0 L$ one finds a condition for the left boundary value of p_{in} for the hysteresis loop

$$\ln \left(\frac{p_{\text{las}}}{p_{\text{in}}} \right) - p_{\text{in}} + p_{\text{las}} = g_0 L. \quad (26)$$

For the right boundary of the loop the maximum of (19) needs to be found. Taking the derivative of this equation with respect to p_1 the following expression for p_{in} is found:

$$p_{\text{in}} = \frac{2p_1^2 - p_{\text{las}}p_1}{2p_1 + 1}. \quad (27)$$

Substituting this condition into (19) yields

$$g_0 L = \ln \left(\frac{2p_1 + 1}{2p_1 + p_{\text{las}}} \right) + (p_{\text{las}} - p_1) \left(\frac{2p_1 + 1}{2p_1 + p_{\text{las}}} - 1 \right) - \frac{2p_1^2 - p_{\text{las}}p_1}{2p_1 + 1} + p_1. \quad (28)$$

ACKNOWLEDGMENT

The authors would like to thank K. Kudo, K. Yashiki, K. Sato, and J. De Merlier from NEC Corporation for lending wave-length-selectable light sources.

REFERENCES

- [1] M. J. Adams and R. Wyatt, "Optical bistability in distributed feedback semiconductor laser amplifiers," *Proc. IEE J. Optoelectron.*, vol. 134, pp. 35–40, Feb. 1987.
- [2] D. N. Maywar and G. P. Agrawal, "Transfer-matrix analysis of optical bistability in DFB semiconductor laser amplifiers with nonuniform gratings," *IEEE J. Quantum Electron.*, vol. 33, no. 11, pp. 2029–2037, Nov. 1997.
- [3] M. Hill, H. de Waardt, G. Khoe, and H. Dorren, "All-optical flip-flop based on coupled laser diodes," *IEEE J. Quantum Electron.*, vol. 37, no. 3, pp. 405–413, Mar. 2001.
- [4] E. Tangdiongga, X. Wang, Z. G. Li, Y. Liu, D. Lenstra, G. D. Khoe, and H. Dorren, "Optical flip-flop: Based on two-coupled mode-locked ring lasers," *IEEE Photon. Technol. Lett.*, vol. 17, no. 1, pp. 208–210, Jan. 2005.
- [5] R. Clavero, F. Ramos, J. Martinez, and J. Marti, "All-optical flip-flop based on a single SOA-MZI," *IEEE Photon. Technol. Lett.*, vol. 17, no. 4, pp. 843–845, Apr. 2005.
- [6] Y. Kim, J. Kim, S. Lee, D. Woo, S. Kima, and T. Yoon, "Broad-band all-optical flip-flop based on optical bistability in an integrated soa/dfb-soa," *IEEE Photon. Technol. Lett.*, vol. 16, no. 2, pp. 398–400, Feb. 2004.
- [7] W. D'Oosterlinck, G. Morthier, R. Baets, and M. K. Smit, "Very steep optical thresholding characteristic using a DFB laser diode and an SOA in an optical feedback scheme," *IEEE Photon. Technol. Lett.*, vol. 17, no. 3, pp. 642–644, Mar. 2005.
- [8] G. Agrawal and N. Olsson, "Self-phase modulation and spectral broadening of optical pulses in semiconductor laser amplifiers," *IEEE J. Quantum Electron.*, vol. 25, no. 11, pp. 2297–2306, Nov. 1989.
- [9] Vpissystems, Inc., vpitransmissionmaker and vpicomponentmaker [Online]. Available: <http://www.vpissystems.com>
- [10] K. Yashiki, K. Sato, T. Morimoto, S. Sudo, K. Naniwae, S. Ae, K. Shiba, N. Suzuki, T. Sasaki, and K. Kudo, "Wavelength-selectable light sources fabricated using advanced microarray-selective epitaxy," *IEEE Photon. Technol. Lett.*, vol. 16, no. 7, pp. 1619–1621, Jul. 2004.



Wouter D'Oosterlinck (S'01) received the degree in electrical engineering from Ghent University, Ghent, Belgium, in 2002. He is currently working toward the Ph.D. degree in electrical engineering at Ghent University.

His research interests include all-optical signal processing using semiconductor optical amplifiers and the modeling and characterization of SOA-based all-optical components.



Geert Morthier (M'93–SM'01) received the degree and Ph.D. degree in electrical engineering from the University of Ghent, Ghent, Belgium, in 1987, 1991, respectively.

From September 1987 until August 1988, he served in the Belgian army. Since 1991, he has been a member of the permanent staff of Ghent University–IMEC. His main interests are in the modeling and characterization of optoelectronic components. He has authored or coauthored over 100 papers in the field and holds several patents. He is also one of the

two authors of the *Handbook of Distributed Feedback Lasers* (Artech House,

1997). From 1998 to end of 1999, he was the Project Manager of the ACTS project ACTUAL dealing with the control of widely tunable laser diodes, and from 2001 to 2005, he was Project Manager of the IST project NEWTON on new widely tunable lasers. In 2001, he was appointed Part-Time Professor at Ghent University, where he teaches courses on optical fiber communication and lasers. He serves on the program committee of several international conferences and is an Editor of *Proceedings IEE Optoelectronics*.



Roel Baets (M'88–SM'96) received the degree in electrical engineering from Ghent University, Ghent, Belgium, in 1980, the M.Sc. degree in electrical engineering from Stanford University, Stanford, CA, in 1981, and the Ph.D. degree from Ghent University in 1984.

Since 1981, he has been with the Department of Information Technology (INTEC), Ghent University. Since 1989, he has been a Professor on the engineering faculty of Ghent University. From 1990 to 1994, he was also a Part-Time Professor with

the Technical University of Delft, Delft, The Netherlands. He has worked mainly in the field of photonic components. With about 300 publications and conference papers as well as about 10 patents, he has made contributions to the design and fabrication of III–V semiconductor laser diodes, passive guided wave devices, photonic integrated circuits, and microoptic components. He leads the Photonics Group at Ghent University–INTEC (which is an associated lab of IMEC), working on photonic devices for optical communication and optical interconnect.

Dr. Baets is a member of the Optical Society of America, the IEEE Lasers and Electro-Optics Society (LEOS), SPIE, and the Flemish Engineers Association. He has been member of the program committees of OFC, ECOC, IEEE Semiconductor Laser Conference, ESSDERC, CLEO-Europe, IPR, and the European Conference on Integrated Optics. He has been chairman of the IEEE-LEOS Benelux chapter from 1999 to 2001.



Thomas Erneux received the Ph.D. degree in chemistry in 1979 from the Free University of Brussels (ULB), Brussels, Belgium.

He studied applied mathematics at the California Institute of Technology in 1979 and Northwestern University in 1980. He became a Professor at Northwestern University, Evanston, IL (1982–1993). He worked on a variety of bifurcation problems mostly in the area of chemical, biological, and laser instabilities. In 1993, he returned to Belgium and became a member of the Theoretical Nonlinear

Optics Group at ULB. His current interests concentrate on laser dynamical instabilities and the applications of delay differential equations in all areas of science. He is currently a full-time research scientist with the Fonds National de la Recherche Scientifique, Brussels.